Chapter 6

Experimental Investigation on the Self-Healing Efficiency of Araldite 2011 Adhesive Reinforced with Thermoplastic Microparticles

Halil Özer and Engin Erbayrak

Additional information is available at the end of the chapter

http://dx.doi.org/10.5772/65167

Abstract

Newly developed self-healing technologies allow self-repair of adhesively bonded joints without the need for replacing the damaged joint with a new one. This study addresses to define experimentally the self-healing ability and efficiency of the Araldite 2011 epoxy adhesive reinforced with the thermoplastic co-polyester (TPC). Heating the joint results in melting the co-polyester in adhesive, and then it is expected to repair the damaged region by the melted co-polyester. Firstly, before applying the self-healing process, a preliminary study was applied to define whether selected adhesive is compatible with the thermoplastic particles in terms of self-healing. From the initial results, it is seen that Araldite 2011 adhesive is suitable for use in the self-healing mechanism. In the healing cycle, initial crack in the reinforced adhesive was propagated until 30 mm during the double cantilever beam (DCB) testing. The fractured specimens were repeatedly healed in terms of the close-then-heal (CTH) scheme until no healing has taken place. After the healing process was completed, the healing efficiency was defined using the fracture energy values. In this study, the healing process was repeated two times with the acceptable healing efficiencies. It is concluded that the damaged reinforced adhesive can repair itself with a considerable healing efficiency.

Keywords: Self-healing, Araldite 2011, Thermoplastic additive, Healing efficiency, DCB test

1. Introduction

Structural adhesives have been used extensively in the space, aviation, automotive, and naval industries. Many techniques have been proposed to reduce high stress concentrations at the lap joints and to improve the joint strength. One of them is adding the additives into adhesive, such as graphene, rubber, nanoparticles, etc. Khan et al. [1] studied the effect of incorporation of different weight fractions of graphene on adhesive mechanical properties. They stated that addition of 0.7 % graphene directly increases both adhesive strength and toughness. In addition, they claimed that the graphene was the most appropriate additive for polyvinyl acetate (PVAc) adhesive. Sadigh and Marami [2] offered the new method of increasing the strength of adhesively bonded joints by reinforcing a small part of reduced graphene oxide (RGO). Finally, they stated that inclusion of 0.5 wt.% RGO increased both ultimate tensile and compressive strength of bulk specimens by rate of 30 and 26 %, respectively.

In addition, an alternative technique has been recently proposed to reduce peel and shear stress concentrations in the lap joints. Different names for this type of joint are used in literature such as mixed-adhesive, modulus-graded, bi-adhesive, and hybrid-adhesive joints. In this technique, stiff and flexible adhesives are used together along the overlap region, without mixing the adhesives. In application of that method, the stiff adhesive is located in the middle and flexible adhesive at the ends of the overlap. Ozer and Oz [3] investigated the effect of the bi-adhesive bondline on the shear and peeling stresses of a double lap joint using a three-dimensional finite element model based on solid and contact elements. Their results show that the stress components can be optimized using appropriate bond-length ratios.

Recently, new technologies proposed to increase the strength and repair the damaged zone of the adhesively bonded joints. Newly developed self-healing technology allows self-heal and self-repair of adhesively bonded joints without the need for replacing the damaged joint with a new one. Banea et al. [4] presented an overview of the recent developments in the use of smart adhesive technology and summarized the different strategies and approaches to obtain smart adhesive joints. The use of self-healing materials in adhesives is also discussed. Yin et al. [5] studied the preparation of epoxy microcapsules by amino resins. In their work, mechanical properties of the epoxy filled with the healing system were evaluated. From the preliminary result of double cantilever beam (DCB) testing, they showed that the plain weave glass fabric laminates using the self-healing epoxy as the matrix received a healing efficiency of 68 %. Long et al. [6] prepared microcapsules with low formaldehyde and evaluated the morphology, mean particle diameter, particle size, wall thickness, mechanical properties, and encapsulation efficiency as compared to microcapsules. They concluded that significant reduction in the levels of formaldehyde content is possible, while only marginally reducing the mechanical properties and still maintaining the encapsulation efficiency of ~75 %. (For more detailed literature on self-healing with microcapsule, see Refs. [5, 7–9].) D'Elia et al. [10] confined their study to a supramolecular polymer in a graphene ultralight network to form robust, electrically conductive composites able to self-repair. They stated that these composites can sense pressure and flexion and fully restore their properties after damage multiple times and without an external stimulus. Chen et al. [11] employed plasma bombardment to introduce

http://dx.doi.org/10.5772/65167

structural defects in monolayer graphene films. They performed thermal annealing to study healing effects on these defects. Luo et al. [12] presented the development of a unique self-adhesive material that maintains a high degree of rigidity at the "adhesive" state while possessing the ability to easily de-bond upon heating. In their study, this adhesive layer can be melted again by heating to easily de-bond, and subsequent rebonding capacity was demonstrated, indicating repeated availability of PCL melt adhesive to the surface by the differential expansive bleeding (DEB) mechanism.

Another method to make self-healing joints for adhesive is to use thermoplastic particles in adhesive. Li et al. [13] modified a thermosetting adhesive by incorporating thermoplastic particles. The prepared joints were fractured per the peel testing of double cantilever beam (DCB) configurations. The fractured specimens were healed in terms of the close-then-heal (CTH) scheme. It is found that the CTH scheme can repeatedly heal the joint with a considerable healing efficiency.

In this study, self-healing efficiency of the Araldite 2011 epoxy adhesive reinforced with the thermoplastic co-polyester (TPC) was experimentally investigated. The weight of the thermoplastic co-polyester was chosen about 10 wt.% of the total composition. Adhesives were cured with two different temperatures including the room temperature (RT) and the temperature above the melting point of the co-polyester. Firstly, for defining the effects of the reinforcement on mechanical properties of adhesives, tensile tests were performed on reinforced and unreinforced dogbone-shaped bulk specimens. Secondly, fracture energy of the unreinforced adhesive was firstly defined from the results of double cantilever beam (DCB) test for Mode I. However, for the adhesive reinforced with TPC, after defining the fracture energy, a 30 mm crack occurred in the reinforced adhesive during the DCB test was closed both by hand and the self-weight of the upper mold, and then the DCB specimen was heated at 120 °C for half an hour in an oven. This fracture healing cycle was repeated until no healing has taken place, i.e., the fractured specimens were repeatedly healed in terms of the close-then-heal (CTH) scheme. After the healing process was completed, the healing efficiency was defined using the fracture energy values of the reinforced adhesive and the self-healed adhesives. In addition, using the Zeiss Evo Ls10 scanning electron microscope, microstructural analyses were also implemented in order to verify whether the co-polyester particles were melted during the healing process. Comparison between our results and the results reported in literature was given.

2. Materials

Material properties of Araldite 2011 adhesive (Huntsman) and co-polyester thermoplastic (Schaetti Fix 376, Switzerland) were tabulated in **Tables 1** and **2**, respectively.

It must be stated that the reason for choosing the co-polyester as additive material is that the lap joint including the co-polyester in adhesive is suitable for repairing the damaged lap joint by heating the joint, as reported in Li et al. [13]. Heating the joint results in melting the co-polyester in adhesive, and then damaged region in adhesive will be repaired by the melted co-

polyester. In this study, the weight of the thermoplastic co-polyester is about 10 wt.% of the total composition, i.e., about 10 wt.% adhesive and co-polyester materials were mixed in a vacuum medium to prevent air bubbles and micro voids using a vacuum device designed and manufactured by authors (**Figure 1**).

		Araldite 2011
Elasticity modulus	MPa	1600
Poisson's ratio		0.41
Tensile strength	MPa	33
Tensile yield strength	MPa	36

Table 1. Mechanical properties of Araldite 2011 adhesive [14–17].

Particle size (μm)	**Density (g/cm³)**	**Melting point (°C)**
80	1.29	109–119

Table 2. Material properties of thermoplastic co-polyester [18].

Figure 1. Vacuum device.

Considering the glass transition temperature (Tg) of Araldite 2011 and the melting point of co-polyester material, curing temperature and times were specified as RT (23 °C)/48 h and 120 °C/7 min from the material data sheets [17, 18]. (Here, RT corresponds to room temperature.) It is seen that the first temperature is below and the second one is above the melting point of the co-polyester.

http://dx.doi.org/10.5772/65167

Secondly, four bulk specimens were prepared for each reinforced and unreinforced bulk specimen accompanied by two different curing temperatures. Therefore, a total of 16 dogbone samples were produced. Then, all four groups of dogbone specimens were cured with two different temperatures (RT and 120 °C). PID-controlled oven was used for curing and self-healing operations. Digital thermocouple was used to record and control the internal temperature of the oven.

Reinforced and unreinforced adhesives were manufactured in a special mold as a thin plate (**Figure 2a**). The plates were then cut into the required dimensions by using KMT waterjet machine (**Figure 2b**). During the cutting process, pressure water (3800 bar) enriched with the abrasive-waterjet-additive sand (80 μ) was used.

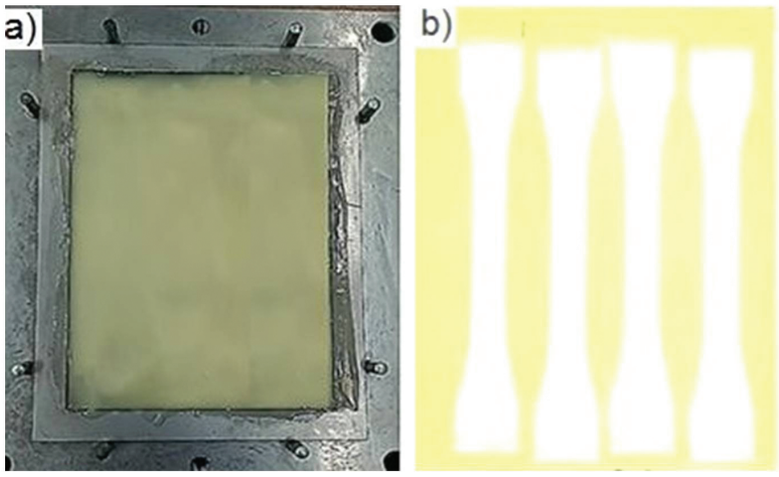

Figure 2. (a) Adhesive sheet within the mold and (b) adhesive sheet with dogbone cutouts.

3. Tensile tests

Reinforced and unreinforced dogbone-shaped bulk specimens were prepared in accordance with BS 2782 standard (**Figure 3**). For each curing temperature, four dogbone specimens were prepared.

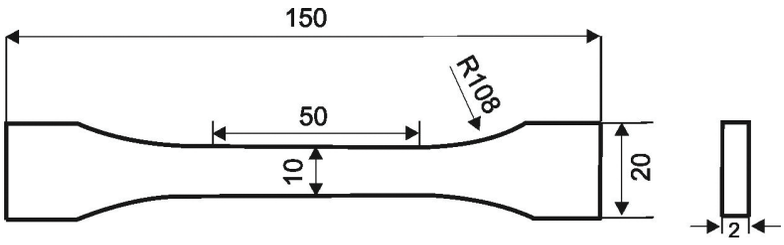

Figure 3. Dogbone specimen (all dimensions in mm).

Tensile tests were performed on test specimens with Instron 5982 at 1 mm/min tensile rate speed (**Figure 4**). The longitudinal strains were recorded during the tests using the video extensometer.

Figure 4. Tensile tester with video extensometer.

Stress-strain curves were obtained both for reinforced and unreinforced dogbone specimens (see **Figure 5**). (In the figure, "unreinforced & RT" corresponds to the tensile test results of the unreinforced adhesive cured at RT.) It is known that Araldite 2011 adhesive is ductile adhesive. As seen in **Figure 5**, under tensile load, the reinforced adhesive has higher deformation capacity than the unreinforced adhesive. Moreover, curing the adhesive at 120 °C causes the adhesive to become more ductile, with respect to curing it at RT. This can be explained by the fact that curing the adhesive at 120 °C results in melting the co-polyester inside the adhesive and leads to increasing the ductility of adhesive. However, as seen in **Figure 5**, the tensile strength is decreasing with increasing the curing temperature. It is concluded that curing temperature and reinforcement effect on the mechanical properties of adhesives.

http://dx.doi.org/10.5772/65167

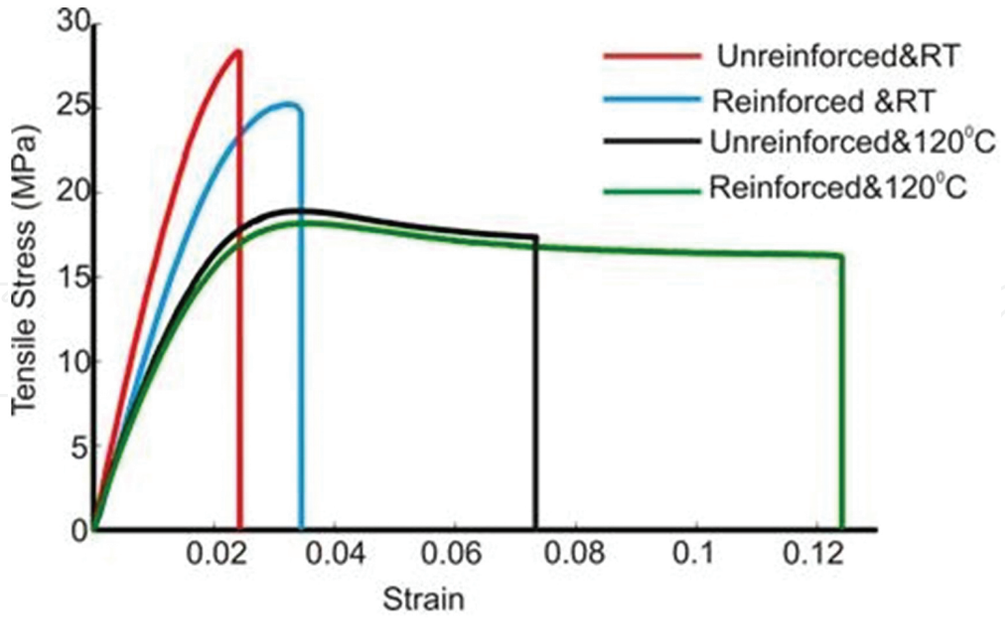

Figure 5. Stress-strain curves of the reinforced and unreinforced specimens cured at RT/48 h and 120 °C/7 min.

In addition, some mechanical properties were presented in **Tables 3** and **4** using the tensile test data of the unreinforced and reinforced dogbone specimens, cured at RT/48 h and at 120 °C/7 min. Comparisons between the mechanical properties were also carried out on the basis of the percent difference. The absolute value of the percent difference is defined as follows:

$$Difference\ \% = \left| \frac{Unreinforced - Reinforced}{Unreinforced} \right| \text{x}100 \tag{1}$$

	Unreinforced	**Reinforced**	**Difference (%)**
Elasticity modulus (MPa)	1667.7	1234.549	25.97
Tensile strength (MPa)	28.351	25.25	10.93

Table 3. Mechanical properties of dogbone samples cured at RT/48 h.

	Unreinforced	**Reinforced**	**Difference (%)**
Elasticity modulus (MPa)	1114.93	1054.331	5.43
Tensile strength (MPa)	18.92	18.20	3.805

Table 4. Mechanical properties of dogbone samples cured at 120 °C/7 min.

As seen in **Tables 3** and **4**, the tensile strengths of the reinforced adhesives are lower than those of the unreinforced ones at the related curing temperatures. In addition, the tensile strength is decreasing with increasing the curing temperature. When it comes to the elasticity moduli, the

elasticity modulus of the unreinforced sample cured at 120 °C is higher than that of the reinforced one with the percent difference of 5.43 % (see **Table 3**). The difference between the moduli was maximum, with the percent difference of 25.97 %, for the dogbone sample cured at RT.

It is reported in literature that the curing temperature has effects on the strength and stiffness of adhesives in relation to their glass transition temperatures (Tg). The Tg value of the Araldite 2011 adhesive cured at RT was reported as 67 °C by DSC method in manufacturer's data sheet [17]. However, the Tg value of the adhesive cured at 120 °C is about in the range between 50 and 60 °C [14]. Therefore, if one compares the variation of the elasticity modulus and tensile strength with respect to the curing temperatures, as seen in **Tables 3** and **4**, curing above the Tg temperature of the unreinforced adhesive results is decreasing in the adhesive strengths and elasticity moduli [14]. However, Tg values of the reinforced adhesive are not available in the open literature and have not also been determined in this study. Despite the lack of the Tg data for the reinforced adhesive, similar decreasing trend was also seen in both the strength and stiffness values of the reinforced adhesive (see **Figure 5** and **Tables 3** and **4**).

As discussed above, a preliminary study was performed to define whether selected adhesive is compatible with the thermoplastic particles. From the initial results, it is seen that Araldite 2011 adhesive is suitable for use in the self-healing mechanism. The self-healing mechanism is discussed in the next section.

4. Self-healing

The fracture energy of the unreinforced adhesive was firstly defined from the results of the double cantilever beam (DCB) test. DCB tests were performed on test specimens with Mecmesin tensile tester at 1 mm/min tensile rate speed. DCB tests were carried out on the configuration depicted in **Figure 6**. An initial pre-crack of 40 mm was introduced to the specimens. The geometric properties of the DCB specimen are as follows: the adherend length $L = 230$ mm, adherend thickness $h = 12$ mm, adherend width $b = 25$ mm, and adhesive thickness $t = 0.2$ mm.

St37 steel was used as an adherend material. The elasticity modulus and Poisson's ratio of the adherend are 210 GPa and 0.3, respectively. It is known that surface treatment mainly affects the strength of adhesively bonded joints [19]. With the help of vacuum blasting machine, sandblasting was applied to the adherend surfaces by using silica carbide sand of size 400 μm. Sandblasted adherend surfaces were cleaned by using an ultrasonic bath in liquid pure acetone. The adhesive thickness between two adherends of DCB specimen was controlled by using the Mylar tape, and the tape of 0.2 mm thickness was fixed on one adherend surface. In **Figure 7**, the adherend surface is seen after performing the sandblasting treatment.

http://dx.doi.org/10.5772/65167

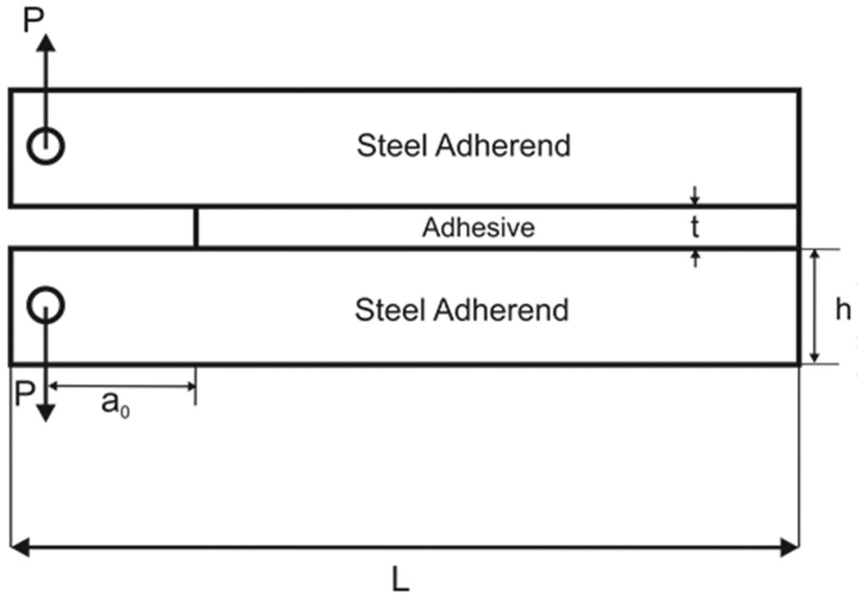

Figure 6. Configuration of double cantilever beam specimen.

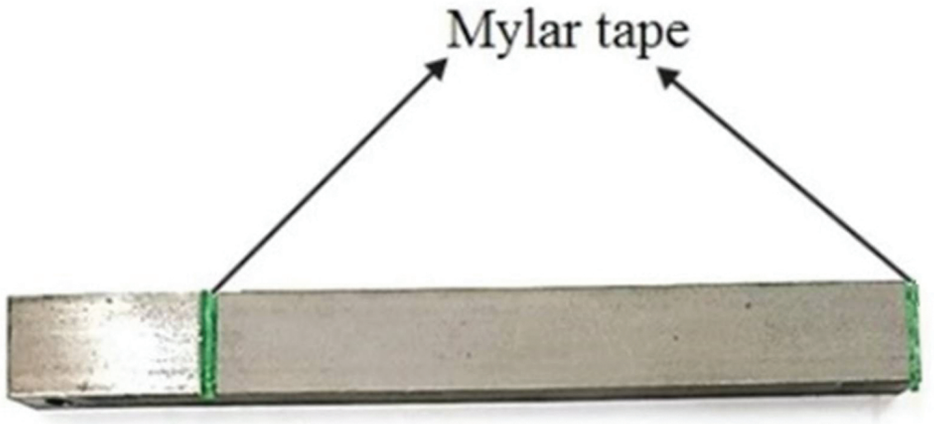

Figure 7. Adherend surface after performing the sandblasting treatment.

In the first stage, also can be named as pre-healing process, fracture energies of the reinforced and unreinforced adhesives were defined from the DCB tests, under the room temperature (23 °C). Tests were continued until the Mode I failure attained.

In the second stage, by following the steps reported in the study of Li et al. [13], when the crack of about 30 mm occurred in the reinforced adhesive during the DCB test, the test was stopped and specimen was removed from the Mecmesin tensile tester. For the four identical DCB specimens, these tests were separately repeated to reach the same crack length of about 30 mm. For measuring and following the crack growth, the adhesive layer over the DCB specimen was painted with the white correction fluid. The DCB specimen test setup is seen in **Figure 8**.

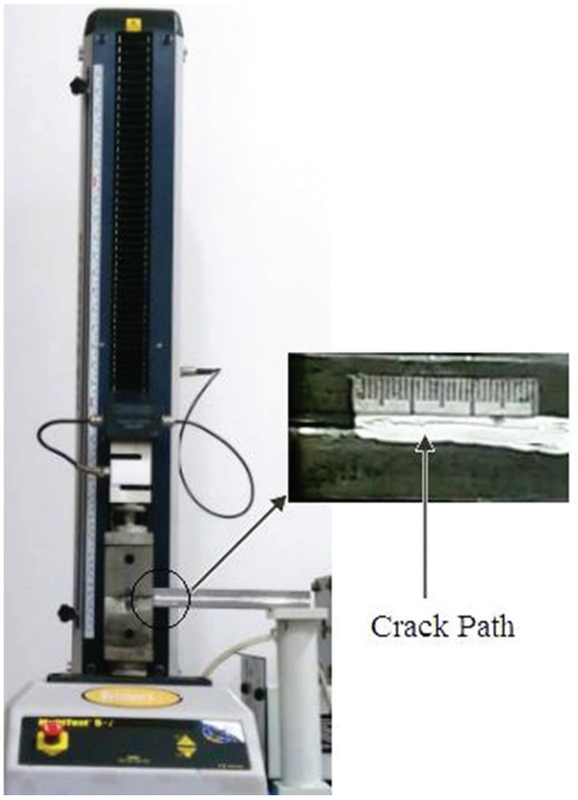

Figure 8. DCB specimen test setup.

After completing the four DCB tests, the first two cracks with the length of 30 mm in two DCB specimens were closed by hand, and the other two cracks having the same lengths were closed by compressive force using the upper part of the mold (self-weight of the upper mold, 45N). The four DCB specimens were then heated at 120 °C for half an hour in an oven and then removed from the oven. It has waited a day to cool the samples to room temperature (RT). By using these four specimens, the DCB tests were performed by continuing tests until the Mode I failure occurred. Loads and corresponding displacements were recorded throughout the tests, and the load-displacement curves were obtained. This cycle is defined the first healing cycle. After the first healing, some cohesive interfacial failures occurred at the adherend surfaces (see **Figure 9**).

Figure 9. Failure surfaces for the DCB specimen.

http://dx.doi.org/10.5772/65167

For the second healing step, new four DCB specimens were prepared again using the reinforced adhesive. For four specimens each, the DCB tests were repeated up to crack reached about 30 mm. After completing the tests, the first two cracks inside the adhesive layer were closed by hand and the second two cracks by the self-weight of the upper part of the mold. The DCB specimens having closed cracks were heated at 120 °C for half an hour in an oven. The specimens were removed from the oven and cooled to room temperature by waiting a day. In this stage, the last process above should be repeated one more time in the next step. Therefore, by using the same specimens, the DCB tests were performed again up to reaching the cracks of about 30 mm; the four cracks were then closed; specimens having closed cracks were secondly cured at 120 °C for half an hour, in which the co-polyester inside the adhesive was melted again by heating; and the specimens were finally removed from the oven and cooled slowly back to RT at a day. Therefore, the last process was repeated twice, without reaching the final crack. The DCB tests were then performed by continuing tests until the Mode I failure attained and the load-displacement curves were obtained using the data of tests. This cycle is named as the second healing cycle.

The healing cycle was repeated until no healing has taken place. In this study, the healing process was repeated two times. The energy release rates (fracture energies) were calculated by using the compliance-based beam method [20] and calculating the area under the load-displacement curve. The healing efficiency was evaluated using the fracture energy values of the reinforced adhesive and the self-healed adhesives. The results were presented and discussed in the next section.

5. Results and discussion

A preliminary study was firstly performed to define whether selected adhesive is compatible with the thermoplastic particles. From the initial results, it is seen that Araldite 2011 adhesive is suitable for use in the self-healing mechanism. The healing process was then started by following the literature procedures [13]. The healing cycle was repeated until no healing has taken place. As stated above, the healing process was repeated two times with the acceptable healing efficiencies. In addition, it is concluded that, during the healing process, closing the crack within DCB specimen by hand gives much better results than closing it by the self-weight of the upper part of mold, in terms of healing efficiency. Aydın et al. [21] experimentally investigated the effect of curing pressure on the strength of adhesively bonded joints. They concluded that the residual thermal stresses occurring due to the curing pressure at elevated temperature need to be taken into account in order to simulate accurately the mechanical behaviors of adhesively bonded joints. Considering that closing the crack within DCB specimen by hand gives much better results, the results presented below are related to closing it by hand, but not closing it by self-weight.

Loads and corresponding displacements were recorded throughout the DCB tests, by continuing the tests until the Mode I failure occurred, and the load-displacement curves were obtained. **Figure 10** shows load-displacement curves. (In **Figure 10**, "unreinforced & DCB"

and "reinforced & DCB" denote the DCB test results of the unreinforced and reinforced adhesives cured at RT. The "first healing" correspond to the DCB test results after performing the first healing cycle.)

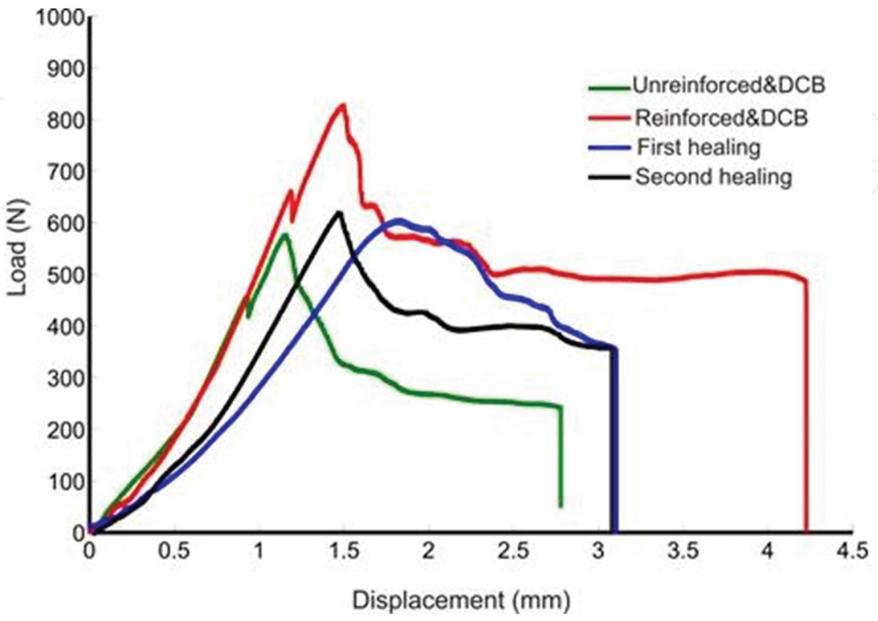

Figure 10. Load-displacement curve.

As seen in **Figure 10**, the reinforced adhesive reaches the highest peak load and has more deformation capacity among all the other. It can be also said that it has also the highest fracture energy, when considering the areas under the curves. Therefore, adding the co-polyester to Araldite 2011 adhesive caused the adhesive to be more ductile than that of the unreinforced adhesive. In addition, it is interesting that the peak load for the adhesive healed twice is higher than that of the unreinforced adhesive. The pick load after the second healing is higher than that of the unreinforced adhesive with the ratio of 7.9 %. From **Figure 10**, it is calculated that the peak displacement value of the reinforced adhesive is higher than that of the unreinforced adhesive by 52 %. Interestingly, the final deformation values remain approximately constant after the first and second healings.

Moreover, the fracture energies were evaluated from the compliance-based beam method, by using the data of **Figure 10** [20]. The main advantage of the method is that there is no need to control the crack lengths during tests. Compliance and flexural modulus values were calculated from the data of **Figure 10**. Using the compliance-based beam method, the fracture energy can be obtained by the relation below [20]:

$$J_{IC} = \frac{6P^2}{hB^2}\left(\frac{2a_e}{E_f h^2} + \frac{1}{5G}\right) \tag{2}$$

http://dx.doi.org/10.5772/65167

where a_e is the equivalent crack length, B the adherend width, h the adherend thickness, G the adherend shear modulus, and E_f the flexural modulus. **Figure 11** shows the fracture energies. (In addition, software built in Mecmesin tensile tester can also automatically calculate the areas under the curves. This gave also the opportunity to check our results.)

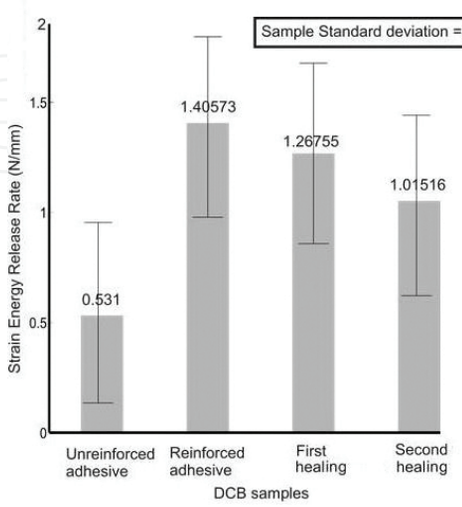

Figure 11. Strain energy release rate values for the DCB samples.

As seen in **Figure 11**, the energy becomes peak for the reinforced adhesive specimen (1.40573 N/mm). The energy is decreasing with increasing the number of healing. It is interesting that the energy at the second healing is approximately two times higher than that of the one at the unreinforced adhesive. In addition, the sample standard deviations of the energy release rates were calculated and given in **Figure 11** [22].

In the final step, the healing efficiency was evaluated using the fracture energy values of the reinforced adhesive and the self-healed adhesives by using the relation below [13]:

$$\eta = \frac{J_{IC}^{\ healed}}{J_{IC}^{\ reinforced}} x100 \tag{3}$$

where J_{IC}^{healed} and $J_{IC}^{\text{reinforced}}$ are the fracture energies of the healed and non-healed reinforced specimens, respectively. From the relation above, it is evaluated that the reinforced adhesive displays 90.166 % healing efficiency after the first healing and 74.812 % after the second healing.

In addition, using the Zeiss Evo Ls10 scanning electron microscope, microstructural analyses were also implemented in order to verify whether the co-polyester particles were melted during the healing cycle (**Figure 12**).

Before curing treatment, the additive TP particles in adhesive can be easily seen in **Figure 12a**. However, when the mixed adhesive was cured at 120 °C, as seen in **Figure 12b**, the co-polyester particles were melted in adhesive.

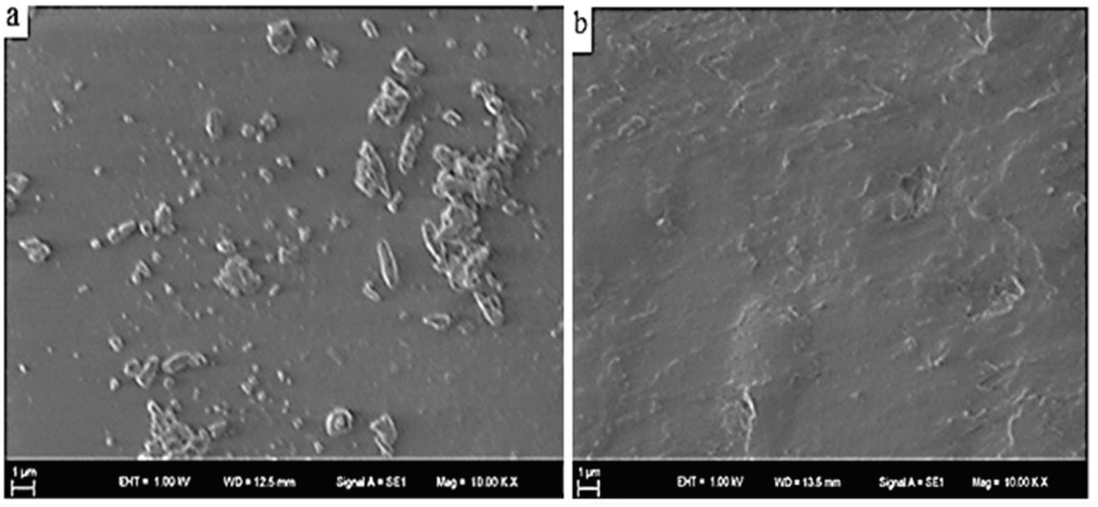

Figure 12. Microstructural view at x 10.000 magnification for the reinforced adhesive (a) cured at RT, (b) cured at 120 °C.

6. Conclusion

Firstly, a preliminary study was applied to define whether selected adhesive is compatible with the thermoplastic particles in terms of self-healing. From the initial results, it is seen that Araldite 2011 adhesive is suitable for use in the self-healing mechanism. Adding the co-polyester to Araldite 2011 adhesive caused the reinforced adhesive to be more ductile than that of the unreinforced adhesive. In this study, the healing process was repeated two times with the acceptable healing efficiencies. Heating the joint resulted in melting the co-polyester in adhesive and allowed the damaged adhesive to repair itself. The following conclusions can be made about the experimental results:

1. The fracture energy is decreasing with increasing the number of healing cycle. The energy at the second healing is approximately two times higher than that of the unreinforced virgin adhesive.
2. The peak load for the adhesive healed twice (i.e., after the second healing) is higher than that of the unreinforced virgin adhesive.
3. During the healing process, closing the crack by hand gives much better results than closing it by the self-weight of the upper part of mold, in terms of healing efficiency.
4. Interestingly, the final deformation values remain approximately constant after the first and second healings.
5. It is concluded that the reinforced adhesive is a reversible adhesive and can repeatedly heal itself with a considerable healing efficiency.

Acknowledgements

This work was funded by Yıldız Technical University under research project no. 2015-06-01-DOP01. The authors would like to thank Professor Hüseyin Üvet, the laboratory director of Yıldız Technical University, for giving the opportunity to use the laboratory facilities.

Author details

Halil Özer* and Engin Erbayrak

*Address all correspondence to: hozer@yildiz.edu.tr

Mechanical Engineering Department, Yıldız Technical University, Istanbul, Turkey

References

[1] Khan U, May P, Porwal H, Nawaz K, Coleman JN. Improved adhesive strength and toughness of polyvinyl acetate glue on addition of small quantities of graphene. Applied Materials & Interfaces. 2013;5:1423-1428. DOI: 10.1021/am302864f.

[2] Sadigh MAS, Marami G. Investigating the effects of reduced graphene oxide additive on the tensile strength of adhesively bonded joints at different extension rates. Materials and Design. 2016;92:36-43. DOI: 10.1016/j.matdes.2015.12.006 0264-1275.

[3] Ozer H, Oz O. Three dimensional finite element analysis of bi-adhesively bonded double lap joint. International Journal of Adhesion & Adhesive. 2012;37:50-55. DOI: 10.1016/j.ijadhadh.2012.01.016.

[4] Banea MD, Da Silva LMF, Campilho DSG, Sato C. Smart adhesive joints: An overview of recent developments. International Journal of Adhesion & Adhesive. 2014;90:16-40. DOI: 10.1080/00218464.2013.785916.

[5] Yin T, Rong MZ, Zhang MQ, Yang GC. Self-healing epoxy composites preparation and effect of healant consisting of microencapsulated epoxy and latent curing agent. Composites Science and Technology. 2007;67:201-212.DOI: 10.1016/j.compscitech. 2006.07.028.

[6] Long Y, York D, Zhangc Z, Preece JA. Microcapsules with low content of formaldehyde: Preparation and characterization. Journal of Materials Chemistry. 2009;19:6882-6887. DOI: 10.1039/b902832c.

[7] Kirkby EL, Michaud VJ, Månsonn JAE, Sottos NR, White SR. Performance of self-healing epoxy with microencapsulated healing agent and shape memory alloy wires. Polymer. 2009;50:5533-5538. DOI: 10.1016/j.polymer.2009.05.014.

[8] Blaiszik BJ, Caruso MM, McIlroy DA, Moore JS, White SR, Sottos NR. Microcapsules filled with reactive solutions for self-healing materials. Polymer. 2009;50:990-997. DOI: 10.1016/j.polymer.2008.12.040.

[9] Jin H, Mangun CL, Griffi AS, Moore JS, Sottos NR, White SR. Thermally stable autonomic healing in epoxy using a dual-microcapsule system. Advanced Materials. 2014; 26:282-287.DOI: 0.1002/adma.201303179

[10] D'Elia E, Barg S, Ni N, Rocha V.G, Saiz E. Self-Healing graphene-based composites with sensing capabilities. Advanced Materials. 2015;27:4788-4794. DOI: 10.1002/adma. 201501653.

[11] Chen J, Shi T, Cai T, Sun TXL, Wu X, Yu D. Self-healing of defected graphene. Applied Physics Letters. 2013;102:103-107. DOI: 10.1063/1.4795292.

[12] Luo X, Lauber KE, Mather PT. A thermally responsive rigid and reversible adhesive. Polymer. 2010;51:1169-1175. DOI: 10.1016/j.polymer.2010.01.006.

[13] Li G, Ji G, Ouyang Z. Adhesively bonded healable composite joint. International Journal of Adhesion & Adhesives. 2012;35:59-67. DOI: 10.1016/j.ijadhadh.2012.02.004.

[14] Carbas RJC, Marques EAS, Da Silva LFM, Lopes AM. Effect of cure temperature on the glass transition temperature and mechanical properties of epoxy adhesives. The Journal of Adhesion. 2014;90:104-119. DOI: 10.1080/00218464.2013.779559.

[15] Zahurul Islam SM, Young B. FRP Strengthened aluminium tubular sections subjected to web crippling. Thin-Walled Structures. 2011;49:1392-1403. DOI: 10.1016/j.tws. 2011.06.007.

[16] Van Tooren MJL, Gleich DM, Beukers A.Experimental verification of a stress singularity model to predict the effect of bondline thickness. Journal of Adhesion Science and Technology. 2012;18:395-412. DOI: 10.1163/156856104323016315.

[17] Hunstman. Araldite 2011 Multi Purpose Epoxy Adhesive [Internet]. 2007. Available from: https://apps.huntsmanservice.com/WebFolder/ui/browse.do?pFileName=/opt/TDS/Huntsman%20Advanced%20Materials/English/Long/Araldite%202011_eur_e.pdf.

[18] Schaetti. High Performance Thermoplastic Copolyester [Internet]. 2015. Available from: http://www.schaetti.com/fileadmin/content/pdf/maerkte_produkte/4_Construction-Bausektor.pdf.

[19] Rudawska A. Selected aspects of the effect of mechanical treatment on surface roughness and adhesive joint strength of steel sheets. International Journal of Adhesion & Adhesives. 2014;50:235-243. DOI: 10.1016/j.ijadhadh.2014.01.032 0143-7496.

[20] De Moura MFSF, Campilho RDSG, Goncalves JPM. Crack equivalent concept applied to the fracture characterization of bonded joints under pure mode I loading. Composites Science and Technology. 2008;68:2224-2230. DOI: 10.1016/j.compscitech.2008.04.003.

[21] Aydın MD, Temiz S, Ozel A. Effect of curing pressure on the strength of adhesively bonded joints. Journal of Adhesion. 2007;83:553-571. DOI: 10.1080/00218460701453536.

[22] Newbold P, Carlson W, Thorne B. Statistics for Business and Economics. 4th ed. New Jersey, USA . Prentice Hall; 1994. 864 p.

IntechOpen